Eur. Phys. J. B **23**, 455–461 (2001)

THE EUROPEAN PHYSICAL JOURNAL B

EDP Sciences

Electronic structure and magnetism of disordered bcc Fe alloys

S. Ghosh[1,a], B. Sanyal[2], C.B. Chaudhuri[1], and A. Mookerjee[1]

[1] S.N. Bose National Centre for Basic Sciences, Kolkata 700091, India
[2] Department of Physics, Uppsala University, Uppsala 75121, Sweden

Received 10 April 2001 and Received in final form 15 August 2001

Abstract. We study the electronic structure and magnetic properties of disordered bcc Co_xFe_{1-x}, Cr_xFe_{1-x} and Mn_xFe_{1-x} alloys in their ferromagnetic phases using the Augmented Space Recursion (ASR) technique coupled with the tight-binding linearized muffin tin orbital (TB-LMTO) method. We calculate the density of states and magnetic moment of these alloys to show the variation upon alloying Fe with the other neighbouring $3d$ transition metals using arguments based on charge transfer, exchange splitting and hybridization effects.

PACS. 71.20.-b Electron density of states and band structure of crystalline solids – 75.50.-y Studies of specific magnetic materials

1 Introduction

Properties of magnetic materials have been a subject of great scientific and practical interest for decades. An enormous amount of experimental and theoretical investigations have been carried out to have a proper understanding of the nature of magnetism in solids [1]. Fe, being one of the ferromagnets among the late transition metals, has drawn considerable attention due to its interesting magnetic properties. Apart from the studies on elemental Fe which include the studies on structural [2] and magnetic phase stability [3–5], there are numerous investigations on magnetism in Fe based ordered and disordered alloys, both theoretically and experimentally. The experimental investigations have provided a variety of information about the magnetic properties of these systems *e.g.* variation of magnetization with band filling [6,7], moment distribution in dilute Fe alloys at low [8] as well as at finite temperatures [9], local environmental effects on magnetic properties [10,11], spatial distribution and thermal variation of hyperfine fields [12], concentration dependence of high field susceptibility [13], low temperature specific heat [14,15] and magnetic phase stability,leading eventually to magnetic phase diagrams [16].

The earlier theoretical studies were based upon various models of band structure calculations [17,18]. Though these calculations were successful to a certain extent in explaining the experimental observations, they suffered from the drawback of having too many adjustable parameters which limited the reliability of their results. However, with recent progresses in first principles electronic structure techniques, the properties of magnetic alloys are investigated more accurately and efficiently. Different aspects of magnetism in both ordered and disordered phases of Fe alloys have been studied successfully by these techniques overcoming the limitations of earlier model calculations [19–22]. In this communication, we aim at a systematic study of electronic structure and magnetic properties of substitutionally disordered Co_xFe_{1-x}, Cr_xFe_{1-x} and Mn_xFe_{1-x} alloys using the self-consistent TBLMTO-ASR technique. In the elemental phase, bcc Fe is a ferromagnet, bcc Cr is a weak non-commensurate antiferromagnet, Mn has a very complicated crystal (unit cell of 58 atoms) and magnetic structure while hcp Co is a ferromagnet. For FeCr, Fe atoms stabilize the commensurate antiferromagnetic (B2) order in the Cr-rich side ($x > 0.8$) although Cr_xFe_{1-x} with $x > 0.8$ are ferromagnets and stabilize in bcc lattice [23]. In case of MnFe alloys, ferromagnetic phase is stable only up to $x = 0.2$ and the crystal stabilizes in bcc lattice. For $x > 0.2$, several phases with antiferromagnetic ordering get stabilized [24]. In FeCo alloys, however, the ferromagnetic phase is stable for the full range of concentrations and the crystal too stabilizes in the bcc structure. To our knowledge, no systematic theoretical study on these three systems has been done so far. This motivated us to perform a systematic investigation of these systems. In this work, we have restricted ourselves only to the ferromagnetic phases of these systems.

2 Theoretical details

We use the methodology of the augmented space recursion technique [25–27] in the first principles framework of the

[a] *Present address:* Department of Physics and Astronomy, Rutgers University, 136 Frelinghuysen Road, Piscataway, New Jersey 08854, USA
e-mail: subhra@physics.rutgers.edu

tight-binding linearized muffin tin orbital method [28]. Extensive details of the description of the methodology have been given in earlier papers [26,27,29]. Therefore, we shall quote here the key results only.

The first order Hamiltonian for a binary random alloy A_xB_{1-x} is represented in TB-LMTO basis as

$$\begin{aligned} H &= \sum_{RL} \underline{C}_{RL} \mathcal{P}_{RL} \\ &\quad + \sum_{RL} \sum_{R'L'} \underline{\Delta}^{1/2}_{RL} S^{\beta}_{RL,R'L'} \underline{\Delta}^{1/2}_{R'L'} \mathcal{T}_{RL,R'L'} \\ \underline{C}_{RL} &= C^{B}_{RL} + \left(C^{A}_{RL} - C^{B}_{RL}\right)\, n_R \\ \underline{\Delta}^{1/2}_{RL} &= \Delta^{B1/2}_{RL} + \left(\Delta^{A1/2}_{RL} - \Delta^{B1/2}_{RL}\right)\, n_R \end{aligned} \tag{1}$$

where $\mathcal{P}_{RL}$ and $\mathcal{T}_{RL,R'L'}$ are the projection and transfer operators in the Hilbert space spanned by the tight binding basis $|RL\rangle$ and n_R is a random occupation variable which is 1 if the site R is occupied by an atom of the A type and 0 if not. C^{Q}_{RL} and Δ^{Q}_{RL} are potential parameters describing the scattering properties of the constituents (Q = A, B) of the alloy and $S^{\beta}_{RL,R'L'}$ is the screened structure constant describing the geometry of the underlying lattice which is nonrandom as we neglect local lattice distortion due to size mismatch of the constituents. The augmented space Hamiltonian replaces the random occupation variable by operators M_R of rank 2. For models without any short-range order,

$$M_R = x\mathcal{P}^{R}_{\uparrow} + (1-x)\mathcal{P}^{R}_{\downarrow} + \sqrt{x(1-x)}\left(\mathcal{T}^{R}_{\uparrow\downarrow} + \mathcal{T}^{R}_{\downarrow\uparrow}\right)$$

is expressed in the basis set vectors formed by linear combinations of the eigenvectors $|0\rangle$ and $|1\rangle$:

$$\begin{aligned} |\uparrow\rangle &= \left(\sqrt{x}|0\rangle + \sqrt{1-x}|1\rangle\right) \\ |\downarrow\rangle &= \left(\sqrt{1-x}|0\rangle - \sqrt{x}|1\rangle\right). \end{aligned}$$

The configuration averaged Green's function $\langle\langle G^{\lambda\sigma}_{LL}\rangle\rangle$ is obtained as a matrix element of the resolvent of the augmented space Hamiltonian in an enlarged basis expressed as a direct product of real space and configuration space bases. $\langle\langle G^{\lambda\sigma}_{LL}\rangle\rangle$ is expressed as a continued fraction expansion by the recursion method. The continued fraction coefficients are exactly calculated up to certain levels of recursion and a suitable terminator is used to approximate the asymptotic part. The local charge densities and magnetic moments are given by

$$\begin{aligned} \rho^{\lambda}_{\sigma}(r) &= (-1/\pi)\Im m \sum_{L} \int_{-\infty}^{E_{\mathrm{F}}} \mathrm{d}E \langle\langle G^{\lambda,\sigma}_{LL}(r,r,E)\rangle\rangle \\ m^{\lambda} &= \int_{r<R_{WS}} \mathrm{d}^3 r\ \left[\rho^{\lambda}_{\uparrow}(r) - \rho^{\lambda}_{\downarrow}(r)\right]. \end{aligned}$$

In our approach, we emphasize the relation between magnetism and charge transfer behaviour. Since in our calculations we have maintained local charge neutrality, we have to deal with the question of strong variation of magnetic moments. Within the itinerant electron theory of magnetism, *this* can be understood in terms of a redistribution of local electronic charge between two spin directions. Together with Coulomb interaction, which determines the positions of the atomic d levels of the constituents and thus the charge transfer in case of a transition metal alloy, magnetic exchange and hybridization play a very important role in determining the magnetic properties. This has already been observed in certain cases [32,33].

These facts can be expressed in a more quantitative form using d-orbital potential parameters $C^{Q}_{d\sigma}$ obtained from TBLMTO for both alloy components (Q=A, B) and for both spin directions (σ =↑, ↓). These quantities are equivalent to the atomic d levels.

The spin dependent diagonal disorder in a random binary alloy A_xB_{1-x} can be defined as [34],

$$\delta_{\sigma} = C^{A}_{d\sigma} - C^{B}_{d\sigma}. \tag{2}$$

The local exchange splitting can be defined as [34],

$$\Delta^{Q}_{e} = C^{Q}_{d\downarrow} - C^{Q}_{d\uparrow}. \tag{3}$$

3 Calculational details

For our calculations we have used a real space cluster of 400 atoms and an augmented space shell up to the sixth nearest neighbour from the starting state. Eight pairs of recursion coefficients were determined exactly and the continued fraction was terminated by the analytic terminator suggested by Luchini and Nex [30]. In a recent paper Ghosh *et al.* [31] have shown the convergence of related integrated quantities, such as the Fermi energy, the band energy, the magnetic moments and the charge densities within the augmented space recursion method. The convergence tests suggested by the authors were carried out to prescribed accuracies. We noted that at least eight pairs of recursion coefficients were necessary to provide Fermi energies and magnetic moments to required accuracy. We have reduced the computational burden of the energy dependent recursion method using the seed recursion methodology [35] with fifteen energy seed points uniformly across the energy spectrum.

Wigner-Seitz radii of the two constituent atoms have been varied in order to have charge neutral spheres. This eliminates the necessity to calculate the Madelung energy which is a difficult task for the case of disordered alloys. Simultaneously we have made sure that the spheres do not overlap too much to violate the atomic sphere approximation (ASA).

The calculations have been made self-consistent within the local spin density approximation (LSDA). The self-consistency cycle was converged in both total energy and charge to errors of the order 10^{-5}. The exchange-correlation potential of von Barth and Hedin [36] has been used, s, p and d orbitals were used to construct the basis functions and scalar relativistic corrections were included. For all the calculations, we have used the lattice constants for the alloys according to Vegard's law. To justify the use

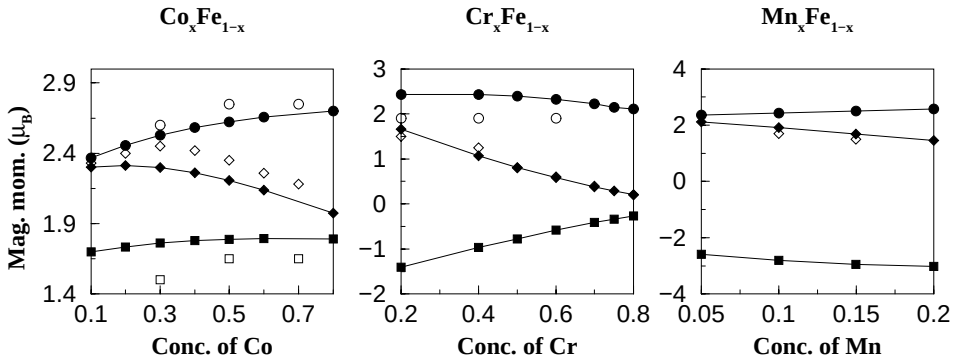

Fig. 1. Partial and averaged magnetic moments (in Bohr-magnetons/atom). In each of the panels, solid line with filled diamonds represents calculated averaged values, the solid line with filled circles represents calculated Fe moments and the solid line with filled squares represent calculated moments of the other constituent. The open diamonds, the open circles and the open squares respectively denote the experimental values of averaged, Fe and other constituent's moments.

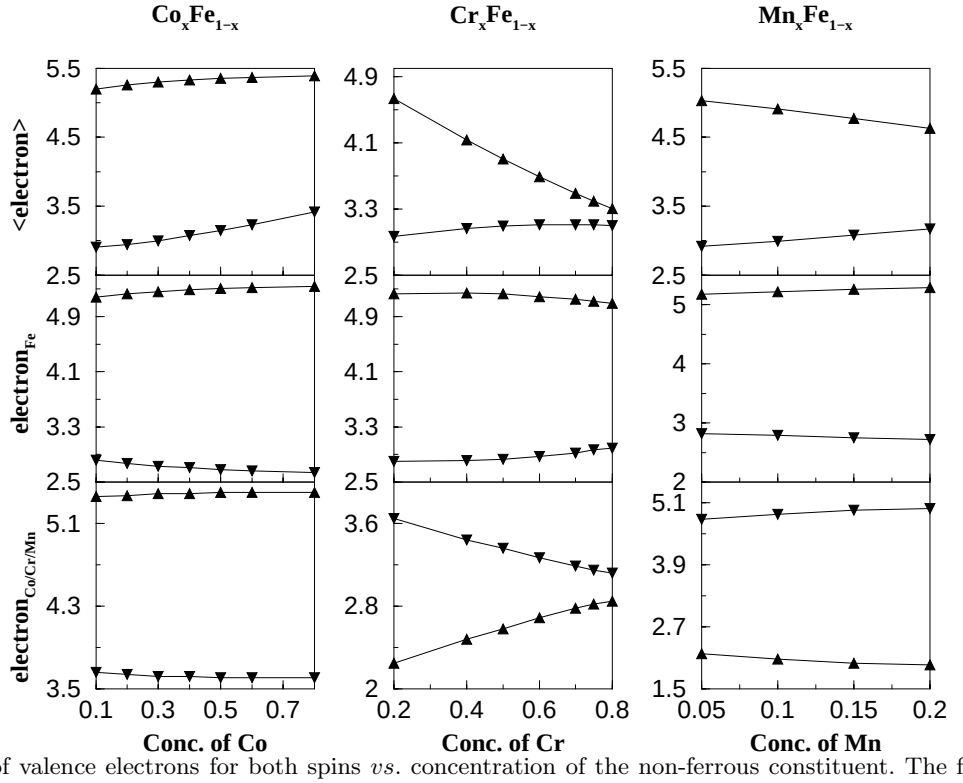

Fig. 2. Number of valence electrons for both spins *vs.* concentration of the non-ferrous constituent. The first row shows the average number of valence electrons for both spins. The second row represents number of electrons at Fe site whereas the third row shows number of valence electrons at Co, Cr and Mn sites. In all the graphs the up and down triangles are for the spin-up and the spin-down electrons.

of Vegard's law, we have also calculated the equilibrium lattice parameters. We have seen that the deviation from Vegard's law is small. Also, the calculated magnetic moments at the equilibrium lattice parameters are within 2% of the Vegard's law values. This is justified as the alloys chosen here contain elements from the same row of the periodic table.

4 Results and discussions

Figure 1 shows the compositional dependence of the local and average magnetic moments for the alloys studied. For Co_xFe_{1-x} alloys, our results agree well with the experiments [7,37]. The results show that the Fe local moment increases with increasing Co content up to $x = 0.3$ beyond which it tends towards a saturation while the Co moment remains almost constant over the whole concentration regime. Similar behaviour has been observed in previous studies using LCAO-CPA [32] and LMTO-CPA [38].

This non-monotonic variation of average magnetization can be explained from the variation of local number of electrons (Fig. 2) and density of states (Fig. 3). In this case, a transition from weak ferromagnetism (incompletely

filled majority d band) for Fe-rich side to strong ferromagnetism (majority d band completely filled) for alloy with a higher Co content ($x > 0.3$) is seen. The initial increase of alloy magnetization corresponds to a continuous filling of majority bands while the minority bands remain almost constantly occupied. The linear decrease of alloy magnetization with increasing x for $x > 0.3$ reflects a strong ferromagnetic region in which majority bands are fully occupied whereas the minority bands accommodate more electrons with increasing Co content. The filling of majority band up to $x = 0.3$ mainly occurs due to incompletely filled majority d band of weak ferromagnet Fe while the rise in the minority band filling beyond $x = 0.3$ is essentially due to a fall in Fe minority electrons and an almost constant nature of Co minority electron number variation (Fig. 2). This is reflected in features of the density of states (Fig. 3). For majority spin states, the filling of d band occurring at Fe sites is accompanied by a steady decrease of DOS at Fermi level n (E_F). Up to $x = 0.3$, the Fermi level is pinned to the minimum of minority spin density of states. Increasing Co content, which essentially means gradual filling, shifts the Fermi level to regions of low spin up density of states and above $x = 0.3$ to increasing spin down density of states. Thus n(E_F) for spin-up decreases while n(E_F) for spin-down increases continuously beyond $x = 0.3$. DOS for ordered FeCo alloy has been calculated by Schwarz and Sahalub [33] by augmented-spherical-wave (ASW) method. The local DOSs for Fe and Co are similar to those of the disordered $Fe_{50}Co_{50}$ alloy studied here except for the fact that due to disorder, the sharp peaks are smeared out. The variation of magnetic moments with concentration of Co is also similar.

All these phenomena are a consequence of local charge neutrality, exchange and hybridization. Since bcc Co is already a saturated ferromagnet, there is hardly any possibility to increase substantially the number of majority spin electrons and hence the local magnetic moment of Co. Because of a small *sp*-density of states at Fermi level compared with the d contribution, the transfer of minority spin d electrons to *sp*-states is expected to be very small. Thus, the Co moment is almost independent of alloy concentration and the possible exchange splitting of Co d level remains almost constant throughout the concentration regime (Tab. 1). On the other hand, the weak ferromagnetism of Fe gives rise to the possibility of filling approximately 0.3 majority spin holes with minority spin electrons. Thus, the local Fe moment increases as a result of increase in local exchange splitting (Tab. 1). Hence, despite being nearest neighbours in the periodic table the exchange makes their behaviour so very different.

The role of hybridization influencing the local magnetic properties can be explained in terms of the bonding charge transfer (BCT) model [39]. As is evident from the density of states, the disorder in the minority spin band is more prominent, which is also realized quantitatively from δ^σ variation. While $\delta^\uparrow$ varies from 40 mRy from Fe-rich side to 6 mRy in the Co-rich side, $\delta^\downarrow$ remains ∼0.8 Ry over the whole range of concentrations. According to the BCT model, different positions of atomic $d^\downarrow$-levels of Fe and Co

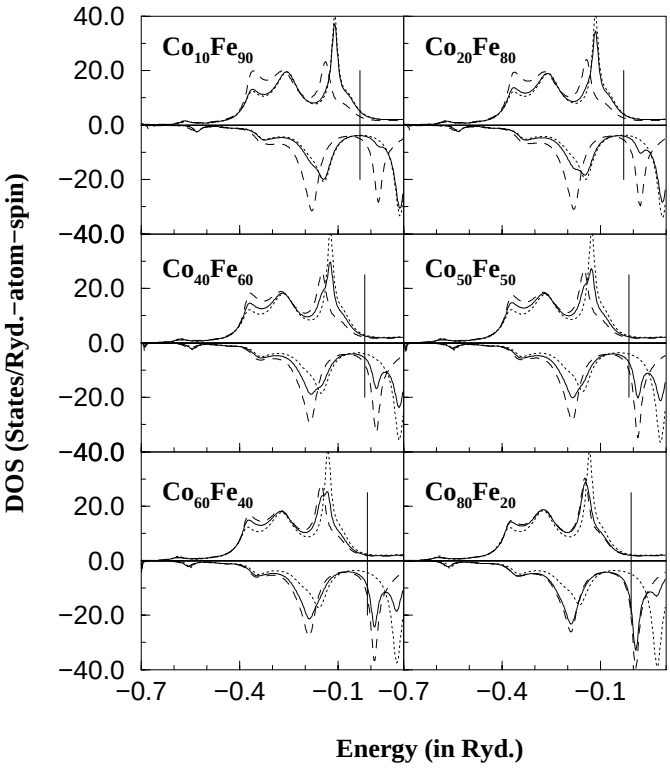

Fig. 3. Spin projected partial and averaged density of states for Co_xFe_{1-x} alloys. In all the cases, the solid line represents averaged density of states while the dashed and the dotted line stand for Co and Fe partial density of states respectively. The vertical lines are the Fermi levels.

Table 1. Local exchange splitting values (in Ry) in Co_xFe_{1-x} alloys with varying concentration of Co.

x_{Co}	Δ_e^{Fe}	Δ_e^{Co}
0.1	0.179	0.136
0.2	0.185	0.139
0.3	0.190	0.140
0.4	0.194	0.142
0.5	0.196	0.142
0.6	0.199	0.142
0.8	0.201	0.138

cause bonding charge transfer (BCT) in the minority spin band. An inspection of the densites of states at various concentrations (Fig. 3) shows that the bonding part of the spin-up density of states has a larger Co weight whereas Fe dominates the anti-bonding part. A transition of minority spin electrons from Fe to Co occurs. To maintain local charge neutrality, mainly Co minority spin electrons are transferred to Fe majority band causing an increase of exchange splitting and magnetic saturation. As a result, a net electron redistribution from $Fe^\uparrow$ to $Fe^\downarrow$ state occurs only to increase Fe moment.

So, to conclude, the magnetization behaviour of CoFe is characterized on the Fe-rich side by the magnetic saturation due to hybridization whereas the Co- rich side is determined simply by a filling of the minority band.

For Cr_xFe_{1-x} alloys our average magnetization results agree well with the experimental values (shown by open diamonds) [43] and other theoretical results [41,42,44]. In fact, for higher Cr concentrations the experimental points almost fall on the theoretical curve establishing good agreement. In case of local moments, our results for Fe agree considerably well with available experimental [44] results but there is quantitative difference in Cr moment values with those of earlier calculations [42,45,46]. In our case, we obtain a larger negative value of the Cr moment which though increases rapidly in the Cr-rich region, never changes its sign,which has been observed in earlier theoretical calculations around $x = 0.7$. However, this slight discrepancy doesn't affect the average properties at all as is seen from the quantitative agreement with the experiments. Even the qualitative nature of the variation of local as well as average moments is well reproduced. As is seen from the figure, the Fe moment remains almost constant up to around $x = 0.4$ and then it decreases in the Cr-rich side but the nature of variation is rather weak. The Cr moment on the other hand increases rapidly as Cr content is increased making the average value to drop down very fast and approaching zero in accordance with the established observation that the average moment collapses around $x = 0.8$ due to a transition from ferromagnetic to antiferromagnetic state.

Once again, we take recourse to the density of states (Fig. 4) and variation of local and average number of electrons as number of valence electrons is decreased (Fe-rich to Cr-rich side) (Fig. 2) to explain such behaviour. A thorough inspection of density of states for various concentrations show that E_F is positioned in a valley between the bonding and antibonding peaks in the minority spin density of states. This feature explains the linear variation of average moment, for, as we keep on increasing Fe content, electrons are added to the majority spin states without affecting much the minority spins. This feature is very clear in Figure 2. The weak variation of Fe magnetic moment can also be explained likewise. The partial Fe density of states for both spins show little variation across the whole range of concentrations whereas the Cr minority density of states varies appreciably as we scan through the concentration regime. This is understandable if one looks into the variation of majority and minority electrons at each site. In the case of Fe, both the majority and minority bands are almost completely filled, while in case of Cr, the majority band accommodates more and more electrons as Cr-content is increased while the minority band loses electrons and eventually they vary in such a way that at a certain critical concentration there will be a greater number of electrons in the majority band. Due to this behaviour of Cr, the average number of up electrons decreases rapidly in contrast to an almost constantly filled minority band in such a way that around $x = 0.8$, the number of electrons in the majority band will be same as that of the minority one, establishing a collapse of magnetic moment when the ferromagnetism to antiferromagnetism transition will take place. Ordered FeCr alloys have been studied in great detail by Moroni and Jarlborg [46].

Table 2. Local exchange splitting values (in Ry) in Cr_xFe_{1-x} alloys with varying concentration of Cr.

x_{Cr}	Δ_e^{Fe}	Δ_e^{Cr}
0.25	0.182	–0.080
0.4	0.179	–0.059
0.5	0.176	–0.047
0.6	0.171	–0.035
0.7	0.163	–0.024
0.75	0.158	–0.020
0.8	0.154	–0.016

Their calculated DOSs for a B2 structure at theoretical equilibrium lattice parameter (5.30 a.u.) are also similar to our Vegard's law calculations for random $Fe_{50}Cr_{50}$ alloy *i.e.* a sharp Fe peak for majority spin and a pseudogap for minority spin.

We investigate now the role of hybridization, exchange etc., and the type of charge distribution within the constraint of local charge neutrality. In Cr, the local exchange splitting varies quite strongly and it increases as Cr content is increased (Tab. 2). The variation in the local exchange splitting for Cr is of the order of 64 mRy from a Fe-rich to a Cr-rich region. This is due to the rapid de-populating of Cr minority band. In Fe, since both the bands are nearly filled, the local exchange splitting does not vary as much like that of Cr. Nevertheless, it decreases,and the variation is of the order of 28 mRy, explaining the decrease of the Fe moment.

The charge-redistribution procedure in this case is quite different. Like FeCo, here the disorder in the minority bands is stronger as is seen from the δ^σ values. $\delta^\downarrow$ varies from 9 mRy to 2 mRy from Fe-rich to Cr-rich side while $\delta^\uparrow$ remains around a value of –0.15 Ry. This stronger disorder in the minority bands indicates a localization of the majority electrons. As is seen from the density of states (Fig. 4), both the bonding and antibonding part of spin down density of states is dominated by Cr. In the case of the majority band, the bonding part is dominated by Fe and antibonding by Cr. Along with this, the nature of variation of the number of electrons for both spins at both the constituents (Fig. 2) suggests that in this case the electron redistribution occurs mainly between $Cr^\uparrow$ and $Cr^\downarrow$ states. Electrons from the Cr minority band migrate to the Cr majority band explaining the rapid increase of the Cr moment.

For Mn_xFe_{1-x} alloys, the experimental results so far available (shown by open diamonds) [40] agree well with our results. Our results also agree to a reasonable extent with calculations based upon Hartree-Fock-CPA [41], but the variation of Mn local moment doesn't agree qualitatively with the KKR-CPA results [42]. In our case the Mn local moment linearly decreases with increasing Mn concentration, a feature that is obtained in Hartree-Fock-CPA calculations too,but the KKR-CPA results predict an opposite trend for Mn moment. The Fe moment weakly increases and the average moment decreases with the Mn

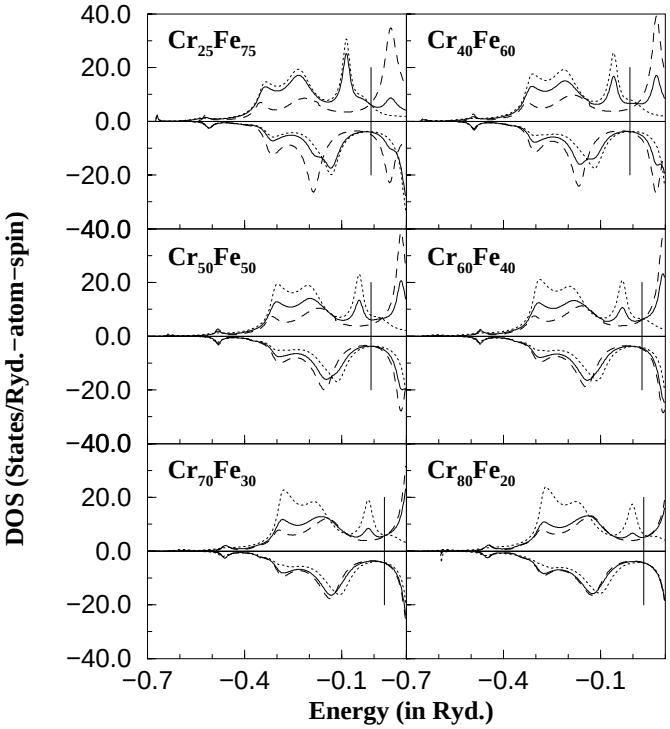

Fig. 4. Same as Figure 3 but for Cr_xFe_{1-x} alloys.

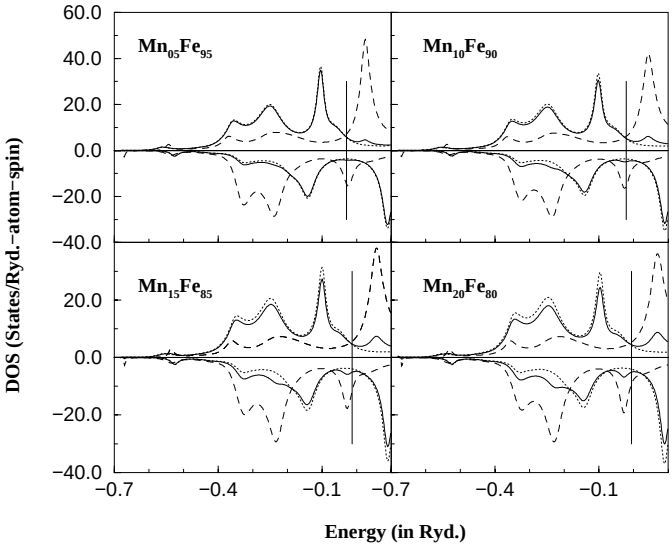

Fig. 5. Same as Figure 4 but for Mn_xFe_{1-x} alloys.

Table 3. Local exchange splitting values (in Ry) in Mn_xFe_{1-x} alloys with varying concentration of Mn.

x_{Mn}	Δ_e^{Fe}	Δ_e^{Mn}
0.05	0.177	–0.170
0.1	0.183	–0.187
0.15	0.188	–0.197
0.2	0.191	–0.202

concentration, which is in qualitative agreement with the experimental Slater-Pauling curve [40].

These variations can be explained once again using band filling arguments and density of states (Fig. 5) plots. Figure 2 shows an almost constantly filled Fe up and down bands across the concentration regime thereby supporting the weak variation in Fe local moment. In case of Mn, the filling accommodates a greater number of electrons in the minority band. As a result, the minority band of the alloy gets gradually filled up while a loss of electrons from the majority bands occurs. For majority spin states, the filling of the majority band at Fe site reduces $n(E_F)$ for the corresponding band, while increasing Mn content shifts the Fermi level to regions of low spin up density of states and high spin down density of states because of a gradual filling of minority electrons.

Once again, these phenomena can be explained on the basis of interplay of local charge neutrality, hybridization and magnetic exchange. Unlike Co, Mn *d* level exchange splitting varies quite considerably (variation of the order of 30 mRy) with Mn concentration due to a gradual filling of the minority band and de-populating of the majority band. As a result, the Mn local moment decreases as one goes to Mn rich region. In Fe, since both the bands are nearly filled, a very weak variation of the number of local electrons is observed. The local exchange splitting variation is of the order of 14 mRy only (Tab. 3). Hence,the Fe local moment increases, though quite weakly compared to Mn.

The role of hybridization and charge re-distribution can be addressed as follows. A close look at density of states reveals that unlike FeCo and FeCr, the disorder is appreciable in both the bands. For the majority band, δ increases up to 50 mRy while $\delta^{\downarrow}$ increases around 8 mRy only. As Mn concentration is increased, the bonding part of spin-up density of states is dominated by Fe while the anti-bonding part is dominated by Mn. The reverse situation is observed for spin down density of states. As a result, majority spins from Mn migrate to Fe and minority spins from Fe migrate to Mn. Thus an increase in Fe local moment is observed. Finally a transition of electrons from $Mn^{\uparrow}$ to $Mn^{\downarrow}$ state occurs reducing the Mn moment gradually.

5 Conclusions

We have studied the magnetism in bcc-based Fe alloys where the three constituents alloyed with Fe belong to the same row of the periodic table and consecutive nearest neighbours of Fe. We have restricted ourselves to the ferromagnetic regions of these alloys only. Our study reveals the very different natures of electronic redistribution among the constituents as we go along from Co to Cr and thus explains the different nature of variation of magnetization in these systems. We have shown the dominant role of hybridization and magnetic exchange under the

constraint of local charge neutrality to explain successfully the variations in magnetic properties of the alloys of nearest neighbours in periodic table.

CBC would like to thank the CSIR, India for financial assistance.

References

1. *Ferromagnetic Materials*, edited by E.P. Wohlfarth, K.H. Buschow, Vol. 1-7 (North-Holland, Amsterdam, 1980-1993).
2. Y. Ishikawa, in *Physics and Application of INVAR Alloys*, edited by H. Saito (Moruzen, Tokyo, 1978).
3. O.K. Andersen *et al.*, Physica B+C **86-88**, 249 (1977); J. Kubler, Phys. Lett. A **81**, 81 (1981); C.S. Wang, B.M. Klein, H. Krakauer, Phys. Rev. Lett. **54**, 1852 (1985).
4. F.J. Pinski *et al.*, Phys. Rev. Lett. **56**, 2096 (1986); U. Gonser, K. Krische, S. Nasu, J. Magn. Magn. Mater. **15-18**, 1145 (1980); Y. Tsunoda, J. Phys. Cond. Matt. **1**, 10427 (1988); V.L. Moruzzi *et al.*, Phys. Rev. B **34**, 1784 (1986).
5. K. Hiraki, J. Phys. Soc. Jpn **58**, 4288 (1989); A.I. Lichtenstein, M.I. Katznelson, V.A. Gubanov, J. Phys. F **14**, L125 (1984); O.N. Mryasov, V.A. Gubanov, A.I. Lichtenstein, Phys. Rev. B. **45**, 12330 (1992).
6. C.G. Shull, M.K. Wilkinson, Phys. Rev. **97**, 304 (1955).
7. D.I. Bardos, J. Appl. Phys. **40**, 1371 (1969).
8. M.F. Collins, G.G. Low, Proc. Phys. Soc. **86**, 535 (1965).
9. H.R. Child, J.W. Cable, Phys. Rev. B **13**, 227 (1976).
10. P. Radhakrishnan, F. Livet, Solid State Commun. **25**, 597 (1978).
11. F. Kajzar, G. Parette, Phys. Rev. B **22**, 5471 (1980).
12. V. Arp., D. Edmonds, R. Peterson, Phys. Rev. Lett. **3**, 212 (1952).
13. J.H.M. Stoelinga, R. Gersdorf, Phys. Lett. **19**, 640 (1966).
14. C.H. Cheng, C.T. Wei, P.A. Beck, Phys. Rev. **2**, 426 (1960).
15. K. Scroder, Phys. Rev. **125**, 1209 (1962).
16. C.M. Van Baal, Physica **64**, 571 (1973).
17. J.C. Mattews, J. Phys. Soc. Jpn **32**, 110 (1972).
18. T. Jo, J. Phys. Soc. Jpn **3**, 794 (1982).
19. P. James *et al.*, Phys. Rev. B **59**, 419 (1999); K. Schwarz *et al.*, J. Phys. F **14**, 2659 (1984).
20. S.K. Burke, B.D. Rainford, J. Phys. **13**, 441 (1983); H. Ebert *et al.*, J. Phys. Cond. Matt. **2**, 443 (1990); F.J. Martinez-Herrera *et al.*, Phys. Rev. B **21**, 1686 (1985).
21. H. Akai, P.H. Dederichs, Phys. Rev. B **47**, 8739 (1993); S. Bluegel *et al.*, Phys. Rev. B **35**, 3271 (1987); I. Turek *et al.*, Phys. Rev. B **49**, 3352 (1994).
22. C. Paduani, J.C. Krause, Phys. Rev. B **58**, 175 (1998); J. Kaspar, D.R. Salahub, J. Phys. F **13**, 311 (1983).
23. N.I. Kulikov, V.V. Tugushev, Sov. Phys. Usp. **27**, 954 (1984); E. Fawcett *et al.*, Rev. Mod. Phys. **66**, 25 (1994); M. Furuska *et al.* J. Phys. Soc. Jpn **55**, 2253 (1986).
24. Y. Endoh, Y. Ishikawa, J. Phys. Soc. Jpn **30**, 1614 (1971).
25. R. Haydock, V. Heine, M.J. Kelly, J. Phys. C **8**, 2591 (1975).
26. T. Saha, I. Dasgupta, A. Mookerjee, Phys. Rev. B **50**, 13267 (1994).
27. B. Sanyal, P. Biswas, A. Mookerjee, H. Salunke, G.P. Das, A.K. Bhattacharyya, J. Phys. Cond. Matt. **10**, 5767 (1998).
28. O.K. Andersen, O. Jepsen, D. Glotzel, *Highlights of Condensed-Matter Theory*, edited by F. Bassani, F. Fumi, M.P. Tosi (North-Holland, New York), p. 59.
29. P.P. Biswas, B. Sanyal, M. Fakhruddin, A. Halder, M. Ahmed, A. Mookerjee, J. Phys. Cond. Matt. **7**, 8569 (1995).
30. M.U. Luchini, C.M.M. Nex, J. Phys. C **20**, 3125 (1987).
31. S. Ghosh, N. Das, A. Mookerjee, J. Phys. Cond. Matt. **9**, 10701 (1998).
32. R. Richter, H. Eschrig, J. Phys. F **18**, 1813 (1988).
33. K. Schwarz, D.R. Salahub, Phys. Rev. B **25**, 3427 (1982).
34. I. Turek *et al.*, *Electronic structure of disordered alloys, surfaces and interfaces* (Kluwer Academic publishers, 1997).
35. S. Ghosh, N. Das, A. Mookerjee, Mod. Phys. Lett. B **13**, 723 (1999).
36. U. Von Barth, L. Hedin, J. Phys. C **5**, 1629 (1972).
37. M.F. Collins, J.B. Forsyth, Phil. Mag. **8**, 401 (1963).
38. I. Turek *et al.*, Phys. Rev. B **49**, 3352 (1994).
39. R. Richter, H. Eschrig, in *Proceedings os the 7th General EPS Conference, Pisa, 1987.*
40. H. Fisher *et al.*, in *Magnetic Ultrathin Films, Multilayers and Surfaces*, edited by A. Fert *et al.* (Materials Research Society, Pittsburgh, 1995).
41. H. Hasegawa, J. Kanamori, J. Phys. Soc. Jpn **33**, 1607 (1972).
42. N.I. Kulikov, C. Demangeat, Phys. Rev. B **55**, 3533 (1997).
43. M.F. Ling, J.B. Staunton, D.D. Johnson, J. Phys. C **7**, 1863 (1995).
44. W.H. Butler *et al.*, J. Magn. Magn. Mater. **151**, 354 (1995).
45. P.H. Dederichs *et al.*, J. Magn. Magn. Mater. **100**, 241 (1991).
46. E.G. Moroni, T. Jarlborg, Phys. Rev. B **47**, 3255 (1993).